DOI: 10.13009/EUCASS2022-7300
9TH EUROPEAN CONFERENCE FOR AERONAUTICS AND SPACE SCIENCES (EUCASS)

Hydrogen-powered propulsion aircraft: conceptual sizing and fleet level impact analysis

Wim Lammen, Bram Peerlings, Elisabeth van der Sman, Johan Kos
Royal Netherlands Aerospace Centre NLR, Anthony Fokkerweg 2, 1059 CM Amsterdam, The Netherlands.
Wim.Lammen@nlr.nl, Bram.Peerlings@nlr.nl, Elisabeth.van.der.Sman@nlr.nl, Johan.Kos@nlr.nl

Abstract
The development of hydrogen-powered aircraft has recently become a topic of major interest, presenting the opportunity to eliminate CO_2 emissions. This paper describes the potential impact of introducing hydrogen (H_2) power, both at aircraft and fleet level. Three passenger aircraft for varying ICAO seat classes were modelled with future entry-into-service (EIS) and with H_2-powered propulsion. The modelling results were applied in a global fleet level analysis with varied traffic development scenarios. The analyses and results in terms of gross energy consumption and emissions (CO_2, NO_X and H_2O) are detailed.

1. Introduction

Anthropogenic climate change and environmental impact are increasingly addressed by governments, international bodies, and industry. In the 2015 Paris Agreement [1], the participating countries set the goal of limiting the global temperature increase well below 2°C above pre-industrial levels and pursuing efforts to limiting this to 1.5°C. This means that net CO_2 emissions should be reduced to zero by 2070 or 2050, respectively [2]. In 2019, the European Commission through its Green Deal announced the objective of Europe to become the first climate-neutral continent by 2050 – a target that has subsequently been implemented in the legally binding European Climate Law [3],[4]. This further stipulates a reduction of CO_2 emissions of 55% across the European industry by 2030, compared to levels in 1990.

For aviation specifically, Europe set environmental goals as part of Flightpath 2050, launched in 2011 [5]. Through successive technology research programmes - such as Clean Sky and Clean Sky 2 (CS2) - Europe is accelerating the progress towards the Flightpath 2050 with high level objectives for reduction of CO_2, NO_X, and noise emissions to be achieved through development of new aircraft and propulsion technologies [6],[7],[8]. Recently, aviation industry's commitments towards net-zero CO_2 have grown, as exemplified in Europe by Destination 2050 [9] and the Clean Aviation Strategic Research and Innovation Agenda [10], and addressed globally by work of the Air Transport Action Group and the International Air Transport Association [11][12].

Recently, the development of hydrogen-powered aircraft has become a topic of major interest, presenting the opportunity to eliminate CO_2 emissions. Hydrogen (H_2) for propulsion cannot be used in current transport aircraft, e.g. because of the absence of adequate H_2 storage systems. Disruptive technologies to enable H_2-powered aircraft are investigated in one of the three pillars in Clean Aviation [10]. Novel aircraft propulsion concepts are being studied either with H_2 combustion engines, H_2 fuel cells (FC) or a combination of both (e.g. [13], [14], [15]). In particular the on-board use of Liquid Hydrogen (LH_2) is under investigation, taking advantage of its more compact storage potential in comparison to compressed Gaseous Hydrogen (GH_2).

The CS2 Coordination and Support Action TRANSCEND [16] (Technology Review of Alternative and Novel Sources of Clean Energy with Next-generation Drivetrains [1]) has investigated what alternative energy sources for aviation and novel aircraft propulsion can contribute to mitigating climate change and achieving the environmental goals for 2050. This paper addresses the potential environmental impact of aircraft propulsion based on H_2 as studied in TRANSCEND. The performance and emission potential were assessed for regional and short medium range (SMR) flights, both at aircraft and fleet level. For three different ICAO seat classes within the 20-300 seats range, H_2-powered configurations were conceptually sized and assessed in terms of mission energy consumption and emissions. Propulsion based on H_2 combustion in gas turbines, on H_2 FC electric power and on combinations of these two using parallel hybrid electric propulsion (HEP), were addressed.

The remainder of this paper is structured as follows. Section 2 summarizes the approach followed for H_2-powered aircraft and fleet modelling. In section 3, the H_2-powered aircraft conceptual sizing process, as well as the main sizing

[1] More information about TRANSCEND is available at the project website, https://project.nlr.nl/transcend/.

DOI: 10.13009/EUCASS2022-7300

and performance results of the three H_2-powered aircraft configurations are explained. Section 4 describes the extension to global fleet level and the corresponding assessments in terms of gross energy consumption and gross emissions, in scenarios with and without the introduction of H_2-powered aircraft configurations. In section 5, the main results, underlying assumptions and limitations of the study are discussed, and section 6 presents conclusions.

2. Modelling approach

This section states the general modelling approach followed to perform the aircraft and fleet level analyses. It describes the applied traffic scenarios (2.1), the H_2 aircraft modelling and extensions to fleet level assessment (2.2), details on H_2 powertrains (2.3) and the applied tooling (2.4).

2.1 Input for the modelling: traffic development scenarios

To assess the impact of introducing H_2-powered aircraft on global, fleet-level scale, two traffic development scenarios were used as input. The scenarios originate from the first assessment of the CS2 Technology Evaluator – from here on referred to as the *DLR CS2 scenarios* [17]. The scenarios mainly differ in terms of growth: in the 'Low' scenario, the number of flights grows from 38 million in 2020 to 56 million in 2050 (+48%). In the 'High' scenario, the number of flights in 2050 has grown to 62 million (+64%). Compound annual growth rate of these scenarios are 1.3 and 1.7%, respectively. As Figure 1 shows, the scenarios start to grow apart from 2035 onwards. Neither scenario includes the impact of COVID-19. Results for 2020-2021 are pre-COVID estimates for those years, rather than actual figures realized.

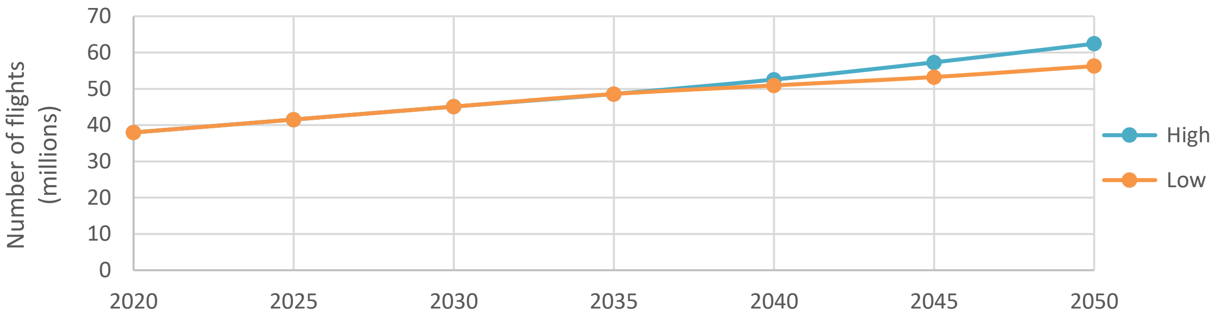

Figure 1: Traffic development (global number of flights) in the two traffic development scenarios considered [17].

Besides a different number of flights, the distribution per seat class differs between the two scenarios. This is shown in Figure 2. In the Low scenario (left), 45% of the total flights in 2050 is operated by aircraft seating up to 210 passengers (81% up to 300 seats); whereas in the High scenario, aircraft seating up to 210 passengers operate 38% of total flights (73% up to 300 seats).

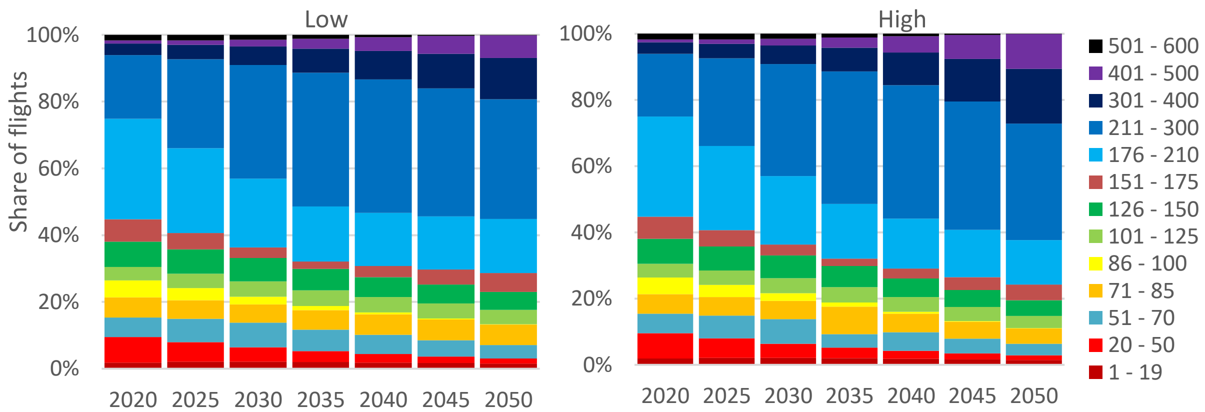

Figure 2: Distribution of flights per seat class, indicated by the colour codes as specified on the right, in the 'Low' and 'High' traffic development scenarios [17].

DOI: 10.13009/EUCASS2022-7300

2.2 Aircraft and fleet modelling

The analysis of the impact of introducing H_2-powered propulsion technology was focussed on aircraft in the 20-300 seats range and applied to regional and SMR flights. For three ICAO seat classes within this seats range, in-service aircraft were selected as reference aircraft, representing the seat class, see Table 1. H_2-powered configurations were derived from these reference aircraft. Future entry-into-service (EIS) years were assumed, taking into account that the applicable H_2 power technology is not available today. In line with the future EIS assumptions general aircraft technology improvements – in terms of weight, aerodynamic drag and specific fuel consumption (SFC) reductions – were applied to the reference aircraft. The modelling of these improvements was based on information from CS2 and other projects ([19],[20],[21]) and was harmonized with expected CO_2 and NO_X emission reductions of future EIS kerosene aircraft as applied in the fleet level assessments, based on the DLR CS2 scenarios[2]. The resulting CO_2 and NO_X emission reductions are depicted in Figure 3 for the improved reference aircraft. The H_2O reductions are similar to the CO_2 reductions, as both these emissions are proportional to the kerosene fuel (and energy) consumption.
The improved reference aircraft were then adapted and conceptually sized for H_2-based propulsion and assessed on their gross emissions and energy consumption. In the sizing, the design payload was kept the same, but the design ranges were shortened compared to the reference aircraft, taking into account expected weight penalties that come with H_2 technology. The design ranges were based on the applied ranges in the DLR CS2 scenarios [17].

Table 1: Modelled H_2-powered aircraft.

Configuration	**Seat class**	**Reference aircraft**	**Reference a/c design range**	**H_2 configuration design range**	**Payload**	**EIS**
Regional	20-50	ATR 42-600	1300 km	1000 km	5.1 t	2035
SMR Single Aisle	151-175	Airbus A320neo	3200 NM	2000 NM	15.9 t	2035
SMR Twin Aisle	211-300	Boeing 787-8	7000 NM	2000 NM	28.6 t	2040

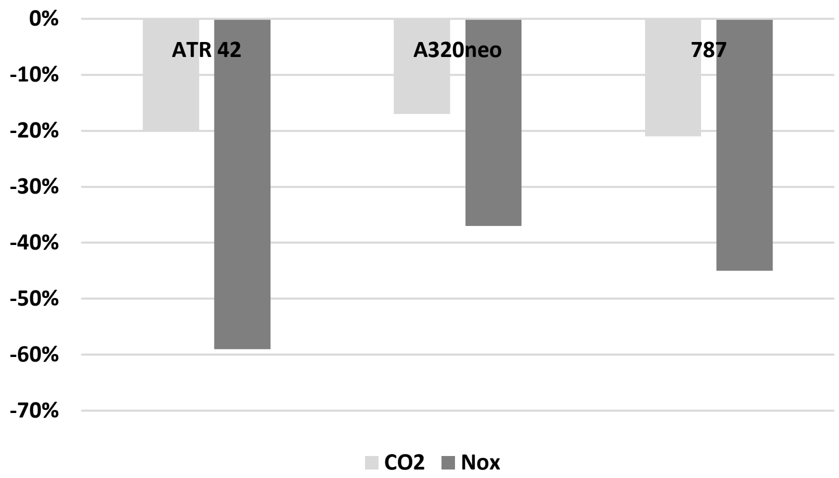

Figure 3: Modelled emission reductions for improved kerosene reference aircraft.

In all H_2-powered concepts, hydrogen was stored in liquid state (LH_2). This the most anticipated storage option for regional and larger aircraft (e.g. [13], [14], [15]) due to its relatively high gravimetric index. Propulsion based on H_2 combustion by gas turbine only, on FC electric power or on combinations of these two (using parallel HEP, see section 2.3) were addressed. H_2 technology performance and sizing parameters were estimated, for a technology level projected at the year 2035. The estimations were based on literature values (e.g. [15]) and on in-house analyses. In addition, these estimations together with other modelling assumptions and preliminary results were reviewed and discussed during a dedicated workshop with experts in the field [18].
For the three H_2-powered configurations, the energy performance and the gross emissions in terms of NO_X and H_2O were calculated for various payload-range combinations and compared with the improved kerosene reference aircraft. The corresponding relative differences (for each payload-range combination) were then applied in the fleet assessments

[2] All aircraft in the DLR CS2 scenarios have expected EIS years and corresponding CO_2 and NO_X emission reductions. These EIS years and reductions are applied to all kerosene aircraft in the fleet level assessments.

DOI: 10.13009/EUCASS2022-7300

for all introduced H_2-powered aircraft in the corresponding seat class. The gross CO_2 emissions, soot emissions, and other carbon gaseous and particle emissions are zero for these aircraft.
The modelling of H_2-powered aircraft was extended to the other seat classes as well, below 300 seats, using the (relative) gross energy and emission results from the three seat classes described above. This is detailed in section 4.
Finally, following the aircraft modelling steps, the impact on global fleets was assessed. Gross emissions and in-flight energy were computed on a flight-by-flight basis, taking into account flight distance between origin and destination and aircraft performance characteristics. Both in the low and high traffic scenarios (see Figure 1), the modelled H_2-powered aircraft in the seat classes 20-300 were introduced for the flights that fit in with the specified payload and range constraints (see Table 1). The fleet level assessment was performed with and without the modelled H_2-powered aircraft.

2.3 Powertrain modelling: hybrid electric propulsion

In the H_2 aircraft modelling, propulsion based on H_2 combustion by the gas turbine, on FC-electric power or on combinations of these two, was addressed. This section zooms in on combined H_2 gas turbine and FC powered propulsion - with parallel HEP - starting from a turbofan or turboprop engine.
In case of a H_2 combustion turbofan, mechanical power assistance can be provided to the fan shaft by an electric motor, to which a fuel cell delivers electric power. This propulsion architecture is illustrated schematically in Figure 4. With the power assistance to the turbofan – especially during peak power phases – the gas turbine engine core can be downscaled slightly, achieving an increased Bypass Ratio (BPR) and therefore an increased propulsive efficiency during cruise. A second advantage of adding the fuel cell is that NO_X emissions can be reduced, as the fuel cell does not emit NO_X. Varying levels of hybridization – determined by the power sizing of the fuel cell - can be applied to the H_2-powered aircraft. Optimization of the sized FC power is described in section 3.1.

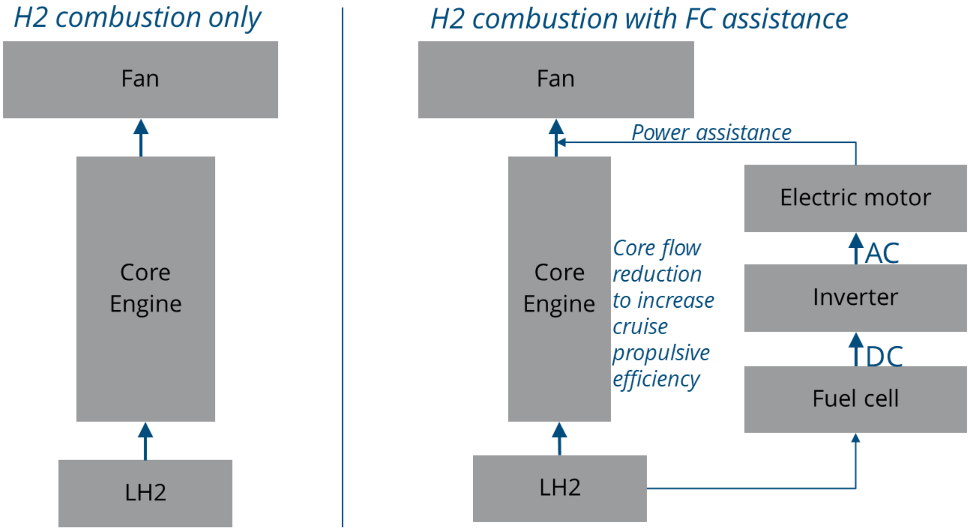

Figure 4: Parallel hybrid propulsion schematic for turbofan.

For the H_2 turboprop case, the effect of HEP was modelled in a different way. Instead of downscaling the engine, an increase of propulsive efficiency was assumed by applying distributed electric propulsion (DEP). DEP units which consist of a propeller, electric motor and inverter, and fuel cell, were assumed. The distributed propeller behavior was not modelled in detail, but its benefits were modelled by increasing the propeller efficiency from 0.8 (standard value [22]) to 0.85[3] in case DEP is applied. In case of the H_2 turboprop – applied with the Regional configuration – HEP variants with gradually increased FC power were applied as well. In this case the FC power was enlarged iteratively until it fully powers the aircraft and turns into an FC-only configuration for which the gas turbines can be removed.

[3] In literature, DEP efficiency values up to 0.9 have been found (e.g. [23]). The value 0.85 was chosen to be a bit more conservative.

DOI: 10.13009/EUCASS2022-7300

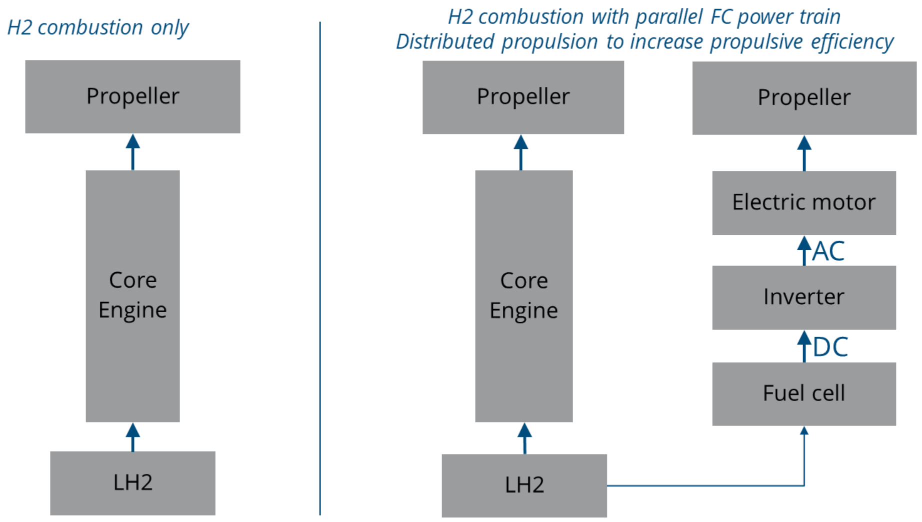

Figure 5: Parallel hybrid propulsion schematic for turboprop.

2.4 Applied tooling

The aircraft modelling and corresponding conceptual sizing and performance analysis was performed using the NLR in-house tool MASS (Mission, Aircraft and Systems Simulation for energy performance analysis [24]), schematically depicted in Figure 6. MASS provides an efficient approach to perform a conceptual sizing and performance simulation of a specified aircraft powertrain configuration, including engines and (HEP) power systems, for a given mission. The fuel flow and total power are calculated as function of mission time in order to predict the total trip energy consumption. Furthermore the engine emissions are calculated. System models of various complexity levels can be applied, depending on the needs. For instance, engine performance models created with NLR's Gas turbine Simulation Program (GSP) [25] can be integrated in MASS.
MASS was used to model and size the H_2-powered aircraft, to evaluate the corresponding energy consumptions and gross emissions for various payload-range combinations and to provide relative differences with the improved kerosene reference aircraft.

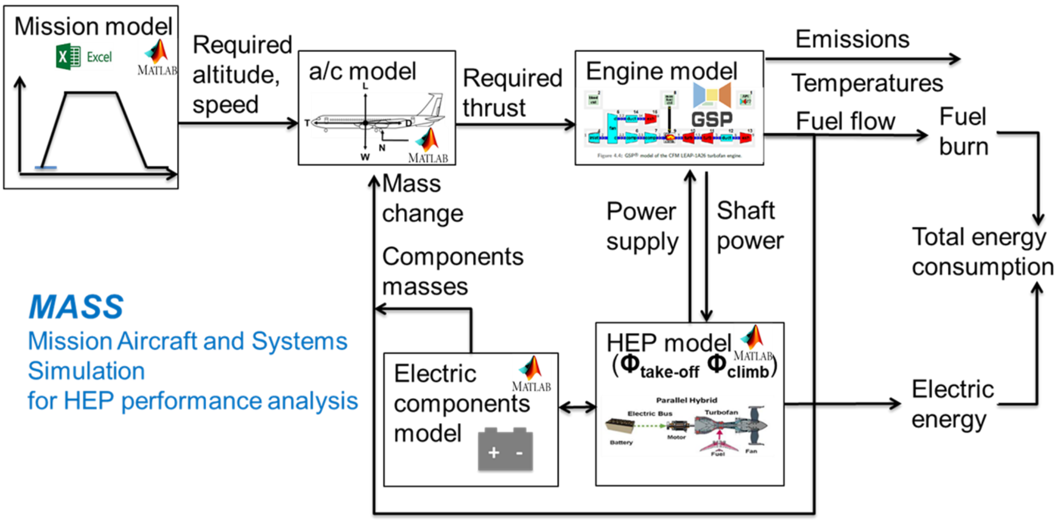

Figure 6: Depiction of the MASS analysis process [24].

The fleet level impact analysis was done using NLR's CO_2-tool, a full-flight gross emissions model based on EUROCONTROL BADA (v3.14) [26] developed for the analysis of flights operated by both existing and future aircraft types. For each combination of origin airport, destination airport and aircraft type, it models a simplified flight profile, based on type-specific performance parameters (e.g. rates of climb and descent, speed, altitude limits). The distance between origin and destination airports is determined from the great circle distance, scaled up by an empirical factor (airport-pair or region-based) to take into account e.g. airspace inefficiencies. For each flight, fuel burn rates are integrated and summed to find total in-flight fuel consumption. These computations take into account the instantaneous

DOI: 10.13009/EUCASS2022-7300

aircraft weight. Initial take-off weights are estimated from default aircraft weight values, based on flight distance. Taxi fuel consumption is determined using default thrust values (7%, per the ICAO emissions databank standard for idle thrust), applied for an airport-specific mean taxi-out and/or taxi-in time [27][28], or default values of 12 and 6 minutes, respectively. Fuel burn for warm-up and cooldown are modelled based again on idle thrust values, for 9 and 3 minutes, respectively. Finally, fuel consumption values for all stages are summed and used to determine CO_2 emissions and energy usage. NO_X emissions were modelled based on the ICAO / EASA emissions databank [29]. No changes in airspace efficiency and ground fuel burn have been assumed towards future years.
Introduction of H_2 aircraft (per seat class) was modelled by applying the relative differences calculated with MASS – in terms of energy and emissions – to all flights that fit in with the feasible payload-range combinations.

3. Aircraft level analysis

The sizing process of the H_2-powered aircraft is explained below in section 3.1 by detailing the SMR Single Aisle case. For the Regional and SMR Twin Aisle cases, a similar process was followed. The overall results are summarized in section 3.2.

3.1 Conceptual sizing of the SMR Single Aisle H_2 aircraft

The sizing process of the H_2-powered aircraft is depicted in Figure 7. First of all, the reference aircraft performance is evaluated for a specific design mission. Next, the reference aircraft design is modified to include new technologies which are expected to be incorporated in new aircraft with an EIS in 2035 (for example lighter materials, improved aerodynamics and lower SFC). The modelling of the new technologies was harmonized – in terms of expected CO_2 and NO_X reduction – with the reductions of the future EIS kerosene aircraft as applied in the fleet level assessments, based on the DLR CS2 scenarios [17], see Figure 3. After that, the modified reference aircraft is further adapted and sized to include H_2-propulsion. All these steps were modelled using the MASS tool, see Figure 6.

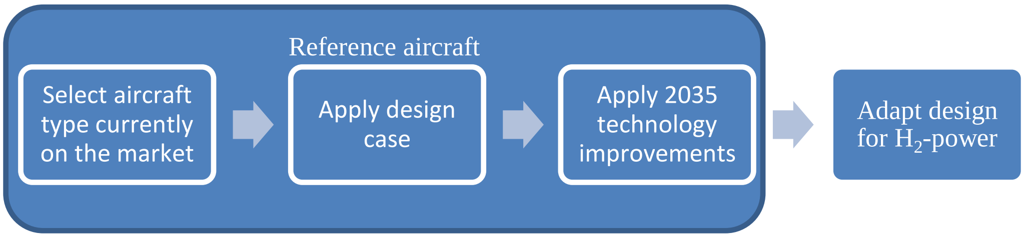

Figure 7: Schematic summary of sizing process.

The modification to H_2-powered propulsion was performed in two parts. First, propulsion based on H_2 combustion by the gas turbine only was modelled. The following assumptions were applied:

- A H_2 Lower Heating Value (LHV) of 120 MJ/kg is applied (kerosene LHV = 43 MJ/kg).
- The LH_2 storage is configured as two cylindric tanks to be placed in the rear fuselage -illustrated in Figure 8 - like in other H_2studies (e.g. [13], [14], [15]). This results in a fuselage extension causing an increase in weight and drag (due to the increase in wetted surface area). It also causes a shift in centre of gravity (CG) for which the wings need to be shifted. The performance impact of the wing shift was not modelled in the sizing evaluations as only a small effect on (trim) drag is expected, e.g. see [30]. An additional small analysis was performed which confirmed this assumption.
- For the sizing of the tanks a gravimetric index (GMI) of 0.35 was applied, in line with [15] for the short range configuration. GMI represents the ratio of the LH_2 fuel mass to the total storage mass:

$$GMI_{Tank} = \frac{m_{LH2}}{m_{LH2}+m_{Tank}} \quad (1)$$

- The fuel mass (either kerosene or H_2) consists of fuel burn and reserve fuel. A 3t reserve fuel mass – taking into account diversion, contingency and loiter was applied for the reference aircraft (Airbus A320neo). This value was adjusted for the sequential configurations, approximately proportional to their mission fuel burn.
- A fixed usable fuel fraction of 0.91 of the total LH_2 fuel stored in the tanks was applied in line with [15] for the short range configuration.

DOI: 10.13009/EUCASS2022-7300

- For the determination of the total tank volume a LH_2 density of 65 kg/m^3 was applied[4]. An additional volume of $0.75m^3$ per tank was reserved for tank systems, and 20 cm separation space between the (inner) tanks fuselage skin as well as 20 cm in between the two tanks was applied (based on in-house estimations).
- For the turbofan engine behaviour a performance model of the CFM Leap was applied [31] based on GSP [25]. No change in thermal efficiency was assumed for the H_2 combustion engine. For the NO_X emission the same performance as with the 2035 kerosene engine was assumed (see also section 5), corrected for the actual power and fuel flow demand.
- H_2 modifications increase the Operating Empty Mass (OEM) and therefore impact the required lift, especially during landing. In the sizing evaluations the lift coefficient (CL) during landing is monitored and checked that it does not exceed the C_L based on the maximum landing mass (MLM) of the A320neo:

$$C_L < 1.92 = \frac{MLM \times g}{S_{wing} \times {}^1\!/_2 \rho v^2} \quad (2)$$

  (with g gravity constant, S_{wing} the wing reference area, ρ the air density and v the true air speed during landing). Otherwise the wing area needs to be resized High-lift systems enhancements are beyond the scope of this study.
- The engine load is checked by monitoring the maximum value of the turbine inlet total temperature (TT4).

The results of the design hypothesis with "H_2 combustion-only" – based on the assumptions described above – are provided in iterative steps in Table 2. After adapting the A320neo to the chosen mission (step 1) and applying the 2035 technology assumptions (step 2), the H_2 powertrain is included. The sizing of the H_2-powered aircraft is derived by following four additional iterative steps, each one adding detail to the sizing. In step 3, H_2 combustion is applied without adding the LH_2 tank mass. In step 4, the tank mass is included based on the tank GMI. In step 5, the fuselage extension (due to the cylindric tank positioning in the rear fuselage) is taken into account only in terms of additional mass. In step 6, also the increased drag due to additional wetted surface area is included in the modelling. The model output parameters are presented in terms of aircraft masses - operating empty mass (OEM), tank mass and GMI, fuel burn, applied reserve fuel and take off mass (TOM) - energy consumption (absolute and relative to the reference aircraft), landing performance (C_L), engine load (TT4), and NO_X emissions relative to the reference aircraft.

Table 2: Evaluation results of the stepwise process for the SMR single aisle "H_2 combustion only" configuration sizing.

Sizing steps	**OEM [t]**	**LH_2 tank mass [t]**	**LH_2 tank GMI**	**Fuel burn [t]**	**Reserve fuel [t]**	**TOM [t]**	**Energy [MWh]**	**Energy [%]**	**Landing max(CL)**	**max TT4 [K]**	**NO_X%**
A320neo: 2000 NM + 3t reserve	44.3			11.1	3	74.3	132.8	100%	1.72	1797	100%
2035 improvements	41.8			9.2	2.4	69.3	110.0	83%	1.63	1770	63%
H_2 combustion	41.8	0	1	3.2	0.9	61.7	105.7	80%	1.59	1740	59%
With tank sizing	50.5	8.7	0.35	3.4	0.9	70.7	114.0	86%	1.83	1775	67%
With tank sizing and fuselage extension (mass)	52.3	8.9	0.35	3.5	0.9	72.5	115.9	87%	1.87	1783	68%
With tank sizing and fuselage extension (mass + drag)	52.9	9.4	0.35	3.7	0.9	73.4	124.1	93%	1.89	1793	75%

From Table 2 it follows that the 2035 kerosene configuration has energy and NO_X reductions of 17% and 37% respectively. This corresponds to the CO_2 and NO_X reductions specified in the DLR CS2 scenarios [17], see also Figure 3, taking into account that the relative energy consumption corresponds to the relative fuel burn and therefore also to the CO_2 emission in the kerosene case. Furthermore, Table 2 shows that the final "H_2 combustion-only" configuration reduces the design mission energy consumption with 7%, compared to the A320neo reference aircraft. This is a much smaller decrease than the 2035 kerosene configuration has (~17%) compared to the A320neo. Compared to the 2035 kerosene configuration the energy increase is caused by the tank sizing effects, accommodated in a stretched fuselage, resulting in additional weight and drag. Taking into account the "snowball" effects (iterative weight increases due to the tank sizing and aircraft fuel consumption adaptations) the sizing converges to a fuselage extension of ~7.8 m. Due

[4] A lower value than the standard LH_2 density of 71 kg/m^3 was applied (as worst case estimate for varying tank pressures between 1 and 6 bar).

DOI: 10.13009/EUCASS2022-7300

to the energy increase the total NO_X emission is also larger than with the 2035 kerosene configuration. This is expressed by a 25% reduction w.r.t the A320neo, which is a smaller decrease than the 37% NO_X reduction of the 2035 kerosene configuration.

Figure 8: Artist impression of SMR single aisle H_2-powered configuration, showing the LH_2 tanks (aft of the cabin) and fuselage extension.

Second, the effect of adding a fuel cell is analysed. For this, the “H_2 combustion-only” configuration is extended with parallel HEP in which the H_2 turbofan engine is assisted by an electric motor (see section 2.3). The electric power is delivered by a fuel cell. Additional assumptions for the hybrid configurations were made:

- A downscaling of 92% of engine core mass flow is applied. This results in a slightly increased BPR and therefore a slightly increased propulsive efficiency. A minimum level of fuel cell assistance is needed to ensure that the engine load – expressed by the turbine inlet total temperature (TT4) - stays below a maximum value. In this case the value of the reference aircraft simulation is applied as upper limit: 1800 K.
- For simplicity, tank sizes are kept constant throughout the hybridisation with fuel cell. The sizes are inherited from the H_2 combustion-only case.
- Constant fuel cell power is applied during a mission, as long as it is lower than the demanded total power.
- In line with [15] a fuel cell specific power of 2 kW/kg was applied (incl. cooling) as well as a fuel cell stack efficiency value of 60%. The additional power consumption by the FC compressor was modelled separately, as function of mission altitude and FC power demand, decreasing the total FC efficiency (53% during cruise). FC cooling power was not modelled in this case and was assumed to be included in the total efficiency.
- Based on in-house estimations, an electric motor specific power of 10 kW/kg was applied. The same value of 10 kW/kg was also assumed for the inverter, with the electric cables included. Furthermore a total electric efficiency (incl. motor, inverter, cabling losses) of 94% was applied.

Starting from the “H_2 combustion-only” configuration a sequence of hybrid configurations is evaluated with an incrementally sized FC power from 0 (the “H_2 combustion-only” configuration) to 3 MW. The results are depicted as function of sized fuel cell power in Figure 9: in terms of H_2 consumption and NO_X emission, Operating Empty Mass (OEM) and Take-off Mass (TOM), and maximum turbine inlet total temperature (TT4, as indicator of gas turbine maximum load) and cruise thrust specific fuel consumption (TSFC, as indicator of combined gas turbine and fuel cell efficiency). From Figure 9 the following can be derived:

- The OEM and TOM increase with fuel cell power, due to the increased sizes of the additional HEP systems (fuel cell plant, electric motors, power electronics).
- The NO_X emission decreases with increased fuel cell power, as the fuel cells do not emit NO_X.
- The maximum TT4 - as indicator of gas turbine maximum load - decreases with increased fuel cell power, as more power support is available, reducing the engine peak load.
- The TSFC has a step reduction first w.r.t “H_2-combustion-only” case (marked by the * symbol), due to the improved propulsive efficiency caused by the engine core downsizing (see section 2.3), but then increases with fuel cell power. This is because the thermal efficiency of the turbofan engine is still higher than the combined fuel cell plant and electric system efficiencies.
- The H_2 consumption – being an indicator of total energy consumption and H_2O emission – increases with fuel cell power because of the OEM and TSFC increase.

DOI: 10.13009/EUCASS2022-7300

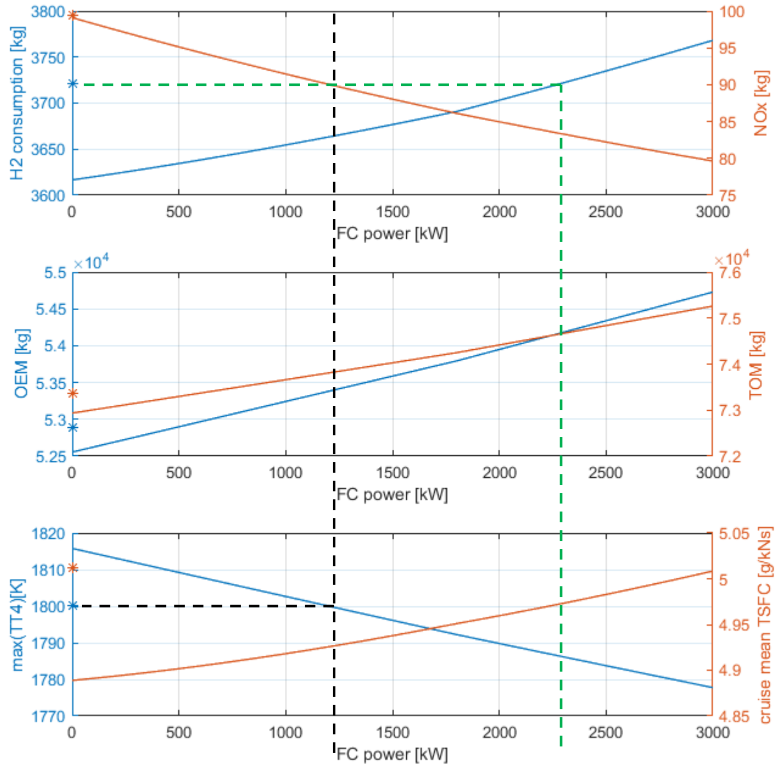

Figure 9: HEP effects as function of FC sized power. The * mark the "H_2 combustion only" configuration

The vertical dashed lines in Figure 9 indicate the optimal fuel cell size with respect to:

- minimal H_2 consumption (black dashed line), with as constraint (represented by the horizontal black dashed line) a maximum engine load below the threshold value (TT4 < 1800 K). This leads to a total FC sized power of 1200 kW.
- minimal NO_X emission (green dashed line), with constraint (represented by the horizontal green dashed line) that the LH_2 consumption is not higher than the (reference) "H_2-combustion-only" case (marked by the * symbols) because of the maximum LH_2 tank capacity. This leads to a total FC sized power of 2300 kW.

In this study the latter is applied as optimal design point: a fuel cell with total sized power of 2300 kW (e.g. implemented by 2 fuel cells of 1150 kW).

3.2 Summarized sizing and performance results all three H_2 aircraft concepts

The sizing of the Regional and the SMR Twin Aisle configurations was performed following the same methods as with the SMR Single Aisle configuration described above, with the following deviations.

- The Regional configuration sizing converged to a propulsion powertrain fully driven by fuel cells. This is caused by the higher efficiency (~55%) of the FC power train compared to the turboprop engines which have low thermal efficiency (a PW127 turboprop model with fixed thermal efficiency of ~30% was applied here). Furthermore, a DEP setup was assumed (see section 2.3).
- The SMR Twin Aisle was based fully on propulsion by H_2 combustion in the turbofan engines. The engine performance in this case was based on a GEnx-1B70 model with a fixed TSFC of 14.7 g/kN/s.

Table 3 summarizes the sizing parameter assumptions and results of the three H_2-powered aircraft, in terms of

- the seat class that it represents, with the corresponding reference aircraft;
- the assumed general technology improvements w.r.t the reference aircraft;
- the applied tank sizing assumptions in line with [15];
- the corresponding fuselage extensions;
- wing area adaptation due to increased landing weight;
- the fuel cell sized power (if applicable);
- the aircraft masses following from the sizing mission.

DOI: 10.13009/EUCASS2022-7300

The future EIS aircraft technology improvements were harmonized with the CO_2 and NO_X reductions applied for the improved kerosene aircraft in the fleet level calculations, as explained in section 2.2 (see Figure 3).
In Table 3 it can be seen that the applied GMI increases with the size of the aircraft. These values were comparable to the GMI values applied in [15] and can be motivated by a larger potential tank volume-to-surface ratio for larger aircraft fuselages. The larger fuselage diameter of the 787-8 also results in a shorter fuselage extension than for the A320neo, even though the same design range is applied and the 787-8 has much larger empty weight. The design missions were both the same for the H_2-powered configuration and for the reference aircraft.

Table 3: H2-powered concept sizing parameters and results.

Sizing parameters	**Regional**	**SMR Single Aisle**	**SMR Twin Aisle**
Applicable seat class	20 - 50	151-176	211 - 300
Reference aircraft	ATR 42-600	A320neo	787-8
Future EIS improvements			
Weight reduction	10%	5%	5%
Drag reduction	3%	5%	5%
TSFC reduction	13%	9%	10%
EIS H_2 configuration	2035	2035	2040
H_2 configuration sizing			
Tank GMI	0.3	0.35	0.37
Tank mass [t]	1.6	9.4	14.1
Usable fuel fraction	90%	91%	92%
Fuselage extension [m]	2.7	7.8	6.3
Wing area increase [%]	4%	1%	0
FC total power [kW]	3400	2300	0
MTOM [t]	19.2	74.7	164.9
OEM [t]	13.6	54.2	128.6
Payload [t]	5.1	15.9	28.6
Fuel burn [t]	0.3	3.7	6.2
Fuel reserve [t]	0.2	0.9	1.4
Design range [km]	1000	3704	3704
Cruise altitude [km]	6.1	10.7	11.3
Cruise Mach	0.49	0.78	0.85

Figure 10 combines the payload range constraint diagrams that correspond to the Maximum Takeoff Mass (MTOM) – calculated for the design mission – of the resulting configurations. Both SMR H_2 configurations have the same range potential but with different payloads. The Regional configuration has much smaller payload-range potential, as could be expected for this aircraft category.

DOI: 10.13009/EUCASS2022-7300

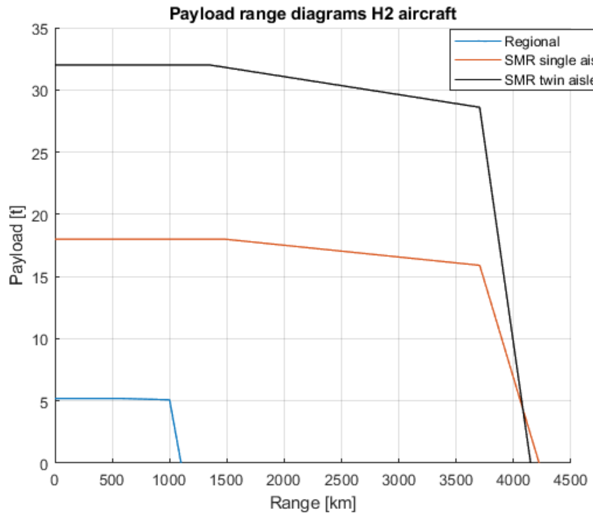

Figure 10: Payload range constraint diagrams for the sized H_2 configurations.

Figure 11 summarizes the energy performance effects of the H_2-powered configurations both w.r.t the current reference aircraft and the improved reference aircraft with future EIS. The margins represent the variations resulting from evaluating various payload-range combinations (within the constraints of the payload-range diagram). Figure 11 shows that the regional configuration has a much lower energy consumption than the SMR configurations. This is caused by the higher efficiency of the FC powertrain compared to the turboprop engines which have low thermal efficiency as described at the beginning of this section. Furthermore the assumed DEP provides an improved propeller efficiency (see section 2.3) and the removal of the gas turbines reduces the OEM. In case of the SMR configurations, the increased weight due to the H_2 power train sizing cannot be compensated by improved efficiencies. Compared to the improved (kerosene) reference aircraft this leads to an increase in energy consumption.

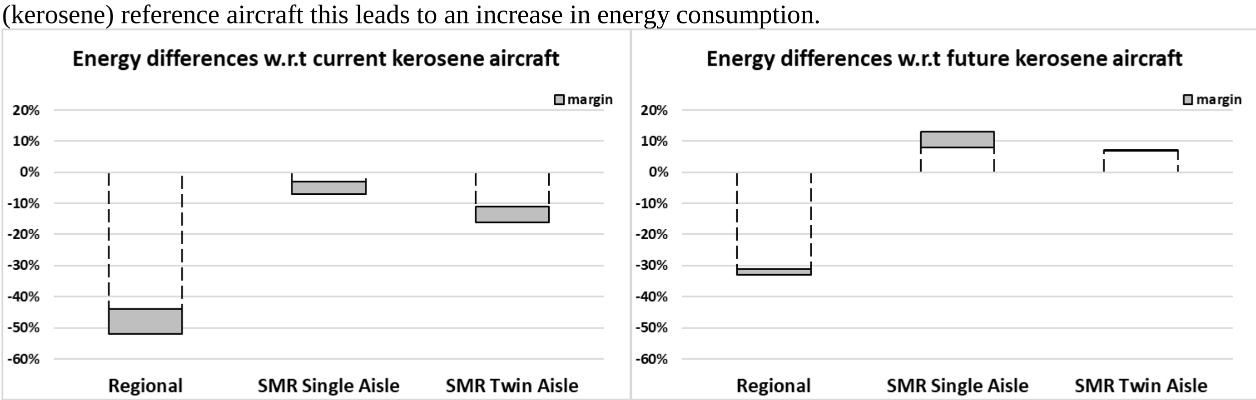

Figure 11: H_2-powered aircraft energy consumption differences w.r.t reference aircraft.

Similar to Figure 11, Figure 12 depicts the NO_X emission effects of the H_2-powered configurations. Here, too, the margins are caused by the variations resulting from evaluating various payload-range combinations.

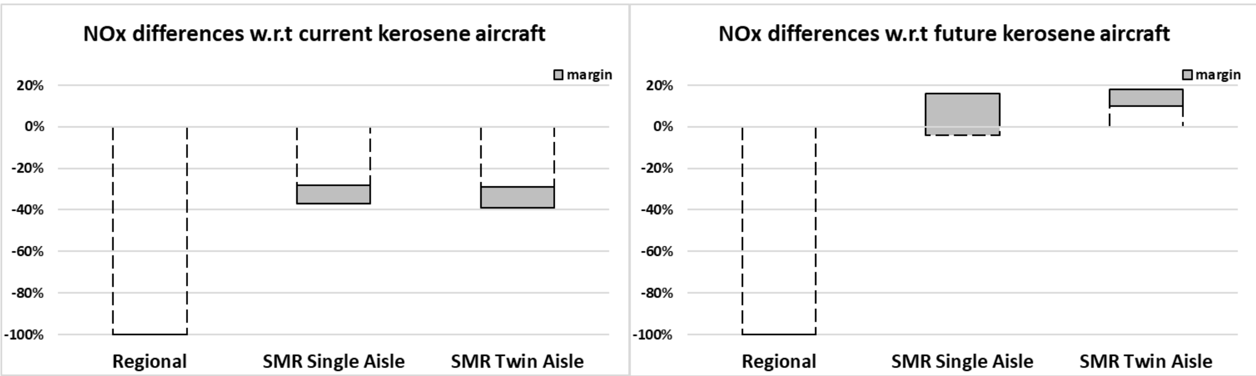

Figure 12: H_2-powered aircraft NO_X emission differences w.r.t reference aircraft.

DOI: 10.13009/EUCASS2022-7300

Figure 12 shows that with the Regional configuration – fully powered by fuel cells – the NO_X emission decreases with 100% (zero NO_X emission by fuel cells). With the SMR configurations, the NO_X emission decreases w.r.t the current reference aircraft, both not w.r.t the improved reference aircraft. This is caused by the increased energy consumption of these configurations (see Figure 11) taking into account that no particular reduction in NO_X emission index was assumed for H_2 gas turbines w.r.t their improved kerosene counterparts (see also section 5).
Finally, Figure 13 depicts the H_2O emission effects of the H_2-powered configurations. All three configurations show a large increase in H_2O emission w.r.t to the reference aircraft and even larger w.r.t the improved reference aircraft. This is inherent to applying H_2 which produces much more H_2O per kg fuel than kerosene [32]. When comparing the three H_2-powered configurations, the same (qualitative) pattern can be seen as with the energy consumption graph: the SMR Single Aisle has the largest relative H_2O increase, directly followed by the SMR Twin Aisle. The Regional aircraft has the smallest relative increase.

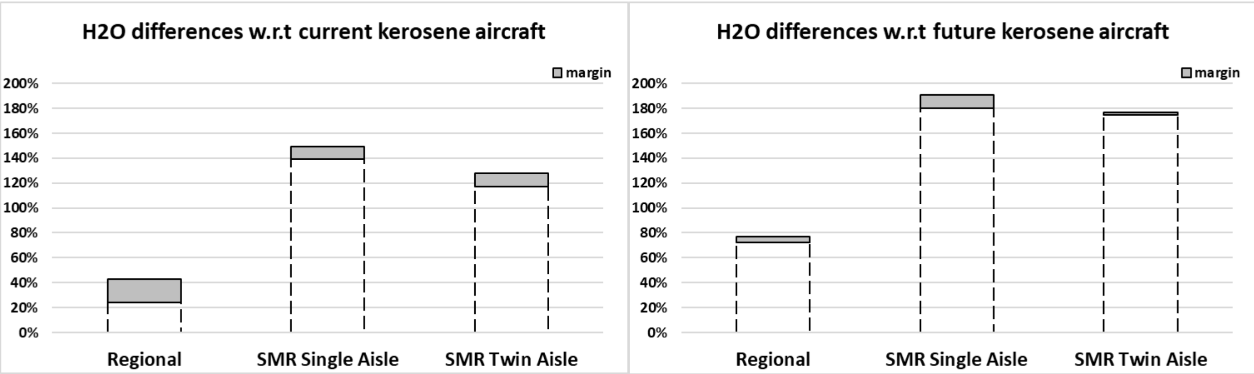

Figure 13: H_2-powered aircraft H_2O emission differences w.r.t reference aircraft.

4. Fleet level impact analysis

The results of the sizing and performance analysis of the three H_2-powered configurations described in the previous section were applied for all introduced H_2-powered aircraft in the corresponding seat class in the fleet assessments. Furthermore, these results were used to estimate the impact of introducing H_2 technology on energy and gross emissions in all seat classes between 50 and 210 passengers, with limited ranges. For various turboprop aircraft seating up to 100 passengers, the corresponding H_2 configuration performance was modelled based on the results obtained from the 20 to 50 seat class (Regional turboprop). For aircraft with capacity for 101 to 210 passengers, the results obtained for the 151-176 seat class (SMR single-aisle turbofan) were used. The seat classes in the DLR CS2 scenarios between 101 and 210 passengers mostly contain turbofan-equipped aircraft with 4, 5 or 6 abreast seating, but also an innovative turboprop seating in seat class 126-150, introduced into service in 2040. Due to the larger size of this aircraft, modelling was still based on the SMR single-aisle turbofan. The combination of interpolation results and the aircraft level modelling for H_2-powered aircraft in the 20-50, 151-176 and 211-300 seat classes supports scenario analysis of H_2-powered aircraft in all seat classes between 20 and 300 seats, for flights that fit within the corresponding payload-range constraint diagram (see Figure 10).
Following the aircraft modelling steps, the impact on global fleets was analyzed. Gross emissions and in-flight energy were computed on a flight-by-flight basis, taking into account flight distance between origin and destination and aircraft performance characteristics. Both in the low and high traffic scenarios (see Figure 1), the modelled H_2-powered aircraft in the seat classes 20-300 were introduced for the flights that fit in with the payload-range constraints (see Figure 10). The fleet level assessment was performed with and without the the modelled H_2-powered aircraft.This analysis was done using NLR's CO_2-tool, a full-flight gross emissions model described in section 2.4. Gross emissions and energy were computed on a flight-by-flight basis, taking into account flight distance between origin and destination and aircraft performance characteristics.
Figure 14 shows the development of energy use and emissions for global aviation in the four cases considered. These are combinations of traffic development scenario (low or high) and the possible use of H_2-powered aircraft (solid or dashed line). Results show that in all cases, global aviation energy use and emissions increase compared to 2020 levels. The impact of H_2-powered aircraft in the low traffic scenario is slightly larger than in the high scenario, because of a higher share of flights in the H_2-applicable seat classes (up to 300 seats), as seen in Figure 2.
Aircraft energy use is mainly governed by the traffic scenario. Higher traffic development results in higher total energy consumption – up from 11 EJ in 2020 to 20 (low traffic scenario) to 24 EJ (high traffic scenario) in 2050. Total aircraft-level energy use is also slightly higher in case H_2-powered aircraft are introduced in the fleet, reflecting findings from the aircraft-level analysis.

DOI: 10.13009/EUCASS2022-7300

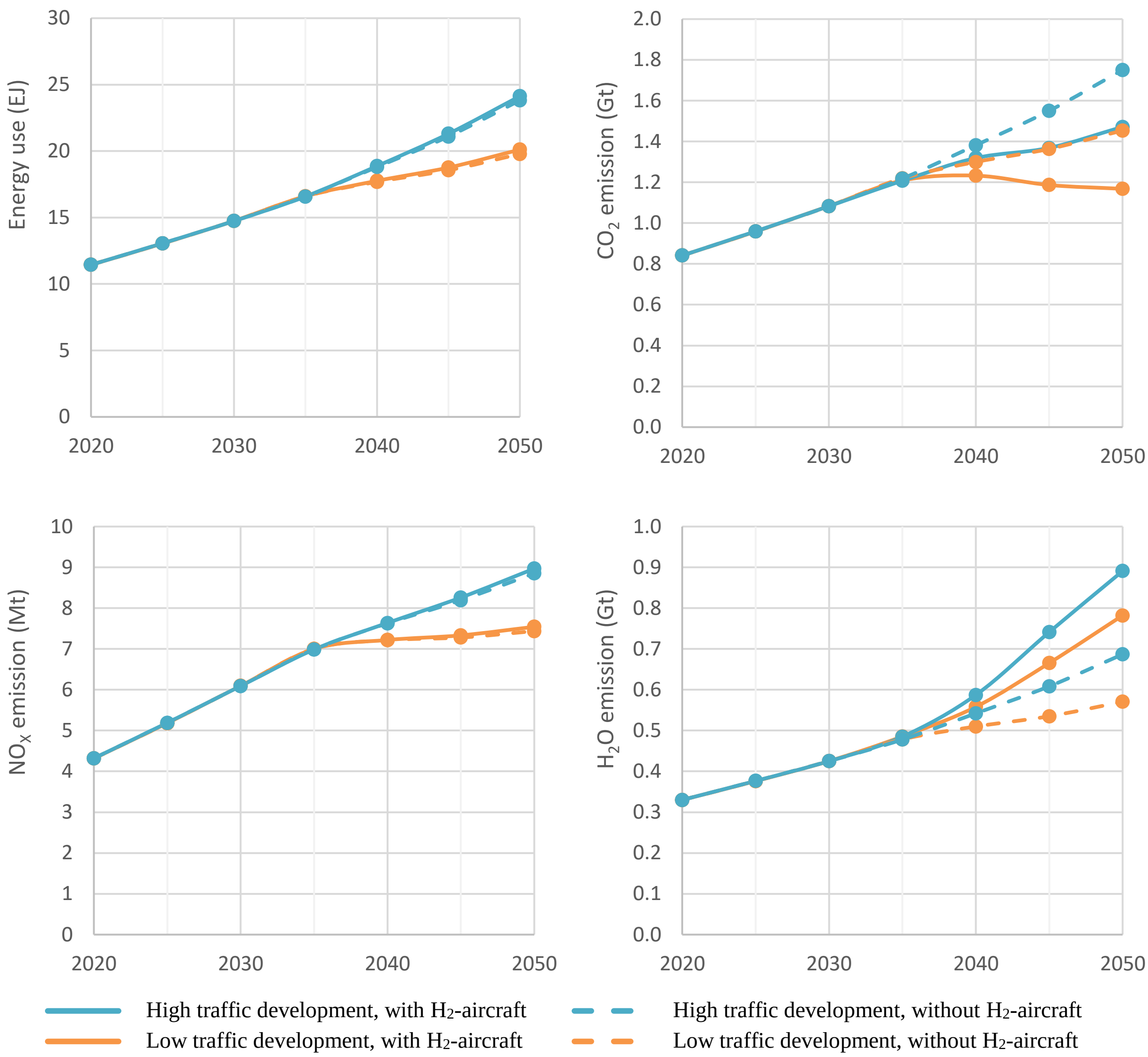

Figure 14: Global aircraft energy use and emissions under high or low traffic development, and with (solid lines) or without (dashed lines) H_2-powered aircraft.

Gross CO_2 emissions are also driven by traffic development, but even more so by the use of H_2-powered aircraft – which have zero gross CO_2 emissions. In the low traffic scenario, the introduction of H_2-powered aircraft helps to stabilize and even reduce global gross CO_2 emissions from 2035 onwards to below 1.2 Gt in 2050. In the high traffic scenario, global gross CO_2 emissions continue to rise to 1.5 Gt in 2050, but less so than if no H_2-powered aircraft were used (1.8 Gt). Clear step changes are observed in 2035 and 2040 in both traffic scenarios, when various H_2-powered aircraft types are introduced.
NO_X emissions again follow the energy use and are slightly increased by the introduction of H_2-powered aircraft. H_2O (water vapour) emissions increase more substantially when H_2-powered aircraft are introduced. Further non-CO_2 climate effects were not studied.

5. Discussion

Several assumptions were made in the aircraft level analysis process, especially for the estimation of the technology parameters related to H_2-powered propulsion. The estimations were based on published values from other H_2-powered aircraft studies (e.g. [15]) and on in-house analyses. However, it remains uncertain how quickly technology will develop before the projected EIS year of 2035. A small uncertainty analysis was performed to determine the parameters with highest sensitivities in relation to the assessment results. From this additional analysis it followed that the tank

DOI: 10.13009/EUCASS2022-7300

sizing parameters (e.g. GMI and volumetric assumptions) as well as the fuel cell efficiency had the most effect on the sizing and performance. These parameter estimations – together with other modelling assumptions and preliminary results – were reviewed and discussed during a dedicated workshop with experts in the field [18]. Consolidated values were retrieved from this workshop and were finally applied in the aircraft and fleet level analyses as described in this paper. Recently, high tank GMI values (above 0.5) were published [33], but these were not taken into in this study.
Initial in-house analysis of H_2 combustion showed that it had little to no effect on the thermal efficiency of the gas turbine. The amount of NO_X reduction however has a large uncertainty, related to various potential assumptions on the combustion chamber (e.g. flame exit temperature, flow distributions). In this study - taking into account the feedback from the expert workshop [18] - the NO_X emission reduction of the H_2 combustion engine has been modelled the same as with the future EIS kerosene reference aircraft (see Figure 3). Other sources [15] suggest 50%-80% NO_X reduction [15] w.r.t current kerosene engines.
The fuel cells (applied on the Regional and SMR Single Aisle configurations) were modelled in a limited way. FC positioning was not taken into account. Only the FC mass penalties – using a fixed specific power estimate – and the performance were modelled. A fixed FC stack efficiency was applied combined with additional compressor losses, modelled as function of mission altitude. With this modelling it was found that the Regional configuration – flying at lower cruise altitude – has a larger total FC efficiency than the SMR Single Aisle. Cooling performance (incl. thermal analysis) was not modelled. A small additional analysis was performed to estimate any potential drag effects resulting from the cooling system. This analysis showed that cooling drag can be ignored in the modelling.
For the Regional configuration the division of the total sized FC power over the multiple propulsion units is not specified yet, because the DEP was not modelled in detail. E.g. it could be four propellers powered by 850 kW fuel cells each or six propellers powered by 567 kW fuel cells each. This would require enhanced modelling of the distributed propulsion system.
Only nominal operation was evaluated, meaning no failure cases were analysed. Although a failure case such as one engine inoperative (OEI) for the SMR configurations would be covered by the inherited design of the reference aircraft for such failure (in combination with the added power from the fuel cell for the SMR Single Aisle), a more detailed analysis of the failure cases would be necessary. For the Regional configuration, the OEI failure will have a smaller impact due to the distributed propulsion system. Nevertheless, additional analysis is recommended here as well.
The H_2-powered configurations were assessed using fixed missions, based on typical missions performed with the corresponding reference aircraft. These missions' characteristics – e.g. the cruise altitude and speed – could be further optimized taking into account the aerodynamic and engine performance and potential emission impact.
Only on-board H_2 aspects were considered so far. The gross CO_2 emissions of the modelled aircraft are zero. This is consistent with assuming the use of so-called green H_2, produced from electrolysis using renewable electricity. H_2 production, supply and demand aspects – also in relation to other alternative fuels for aviation – are not considered in this paper, but have been addressed in TRANSCEND [34]. In general, a holistic approach is recommended to get understanding of the full life-cycle impact of H_2 based propulsion, also for situations where non-green H_2 might be used.

6. Concluding remarks

The gross emission and energy consumption impact of introducing H_2-powered propulsion in future air traffic scenarios was assessed on a global fleet scale. To support this assessment H_2-powered aircraft were modelled for three ICAO seat classes:

- Regional, configuration powered by fuel cells, seat class 20-50, 1000 km range – based on ATR-42 aircraft, with EIS 2035;
- SMR Single Aisle, turbofan configuration with fuel cell HEP, seat class 151-176, 2000 NM range – based on Airbus A320neo aircraft, with EIS 2035;
- SMR Twin Aisle, turbofan configuration, seat class 211-300, 2000 NM range – based on Boeing 787-8 aircraft, with EIS 2040.

The modelling assumptions and preliminary results were reviewed and discussed during a dedicated workshop with experts in the field.
In the fleet level assessments, H_2-powered propulsion was introduced in aircraft replacing the CS2 aircraft concepts in the seat classes 20-300 passengers in flights with short ranges (<1000 km for seat classes 20-100; <2000 NM for seat classes 101-300). The H_2-powered aircraft are introduced in the fleet from 2035 onwards, for single aisle aircraft (seat-classes 20-210) and from 2040 onwards for small twin aisle aircraft (seat class 211-300). The relative amount of simulated flights with H_2-powered aircraft increases up to 38% in the low traffic scenario and up to 35% in the high scenario. This leads to a fleet level reduction of 20% (low traffic scenario) and 16% (high traffic scenario) in global gross CO_2 emissions in 2050 compared to the case without introducing H_2-powered propulsion, whereas global energy

consumption and NO_X emission slightly increase and H_2O emission increases significantly. Application of green H_2 was assumed.

Acknowledgements

- This research has been carried out in the TRANSCEND project, a Coordination and Support Action of Clean Sky 2's Technology Evaluator. This project has received funding from the Clean Sky 2 Joint Undertaking (JU) under grant agreement No 864089. The JU receives support from the European Union's Horizon 2020 research and innovation programme and the Clean Sky 2 JU members other than the Union.
- The German Aerospace Centre DLR is acknowledged for their provision of the "DLR CS2 scenarios".
- David Engler Faleiros and Martijn Blom are acknowledged for their contributions to the fleet assessments.
- Many experts contributed to the expert workshops organised by TRANSCEND for alternative aviation fuels and H_2-powered propulsion. The experts are acknowledged for their valuable feedback on preliminary results provided to them.

Disclaimer

The document reflects only the author's views and the JU is not responsible for any use that may be made of the information it contains.

References

[1] UNFCCC 2015. Adoption of the Paris Agreement. United Nations.
[2] IPCC. 2018. Summary for Policymakers. Global Warming of 1.5°C. An IPCC Special Report on the impacts of global warming of 1.5°C above pre-industrial levels and related global greenhouse gas emission pathways, in the context of strengthening the global response to the threat of climate change. Geneva. Switzerland. World Meteorological Organization. p. 32pp.
[3] EC 2019. The European Green Deal. Brussels.
[4] EC 2020. Proposal for a Regulation of the European Parliament and of the Council establishing the framework for achieving climate neutrality and amending Regulation (EU) 2018/1999 (European Climate Law). Brussels. European Commission.
[5] EC. 2011. Flightpath 2050: Europe's vision for aviation: maintaining global leadership and serving society's needs. Publications Office.
[6] Clean Aviation. 2022. Programme overview and structure. Online: https://www.clean-aviation.eu/clean-sky-2 . [Accessed 10 June 2022].
[7] EC. 2007. Council Regulation (EC) No 71/2007 of 20 December 2007 setting up the Clean Sky Joint Undertaking. Brussels: European Commission.
[8] EC. 2014. Council Regulation (EU) No 558/2014 of 6 May 2014 establishing the Clean Sky 2 Joint Undertaking. Brussels: European Commission.
[9] E. van der Sman, B. Peerlings, J. Kos, R. Lieshout and T. Boonekamp. 2021. Destination 2050: A Route to Net Zero European Aviation. NLR. Amsterdam.
[10] Clean Aviation. 2021. Strategic Research and Innovation Agenda (Version December 2021).
[11] ATAG. 2021. Waypoint 2050 - Second edition. Air Transport Action Group.
[12] IATA. 2021. Net-Zero Carbon Emissions by 2050. Online: https://www.iata.org/en/pressroom/2021-releases/2021-10-04-03/ [Accessed 10 June 2022].
[13] Airbus ZEROe. 2021. Online: https://www.airbus.com/en/innovation/zero-emission/hydrogen/zeroe [Accessed 10 June 2022].
[14] FlyZero. 2022. Online: https://www.ati.org.uk/flyzero/ [Accessed 10 June 2022].

DOI: 10.13009/EUCASS2022-7300

[15] McKinsey & Company. 2020. Hydrogen-powered aviation A fact-based study of hydrogen technology, economics, and climate impact by 2050.Online: 20200507_Hydrogen Powered Aviation report_FINAL web (ID 8706035).pdf (europa.eu) [Accessed 10 June 2022].
[16] J. Kos, P. Osseweijer, T. Zill. 2020. European TRANSCEND for Novel Aircraft Propulsion and Alternative Fuels Roadmaps towards 2050. *Aerospace Europe Conference. Bordeaux. 25-28 February 2020*. NLR-TP-2020-171.
[17] M. Gelhausen, W. Grimme, A. Junior, C. Lois, & P. Berster. 2022. Clean Sky 2 Technology Evaluator—Results of the First Air Transport System Level Assessments. *Aerospace. 9(4). 204*. doi:10.3390/aerospace9040204.
[18] NLR. 2021. Hydrogen-powered propulsion workshop. Online: https://project.nlr.nl/transcend/hydrogen-powered-propulsion-workshop/ [Accessed 10 June 2022].
[19] A. Leipold, et al. 2021. DEPA 2050 – Development Pathways for Aviation up to 2050 (Final Report). German Aerospace Center.
[20] Clean Sky 2. 2021. Technology Evaluator First Global Assessment 2020 Technical Report. Online: Technology Evaluator First Global Assessment 2020 Technical Report | Clean Aviation (clean-aviation.eu) [Accessed 10 June 2022].
[21] P. Schmollgruber, D. Donjat, M. Ridel, I. Cafarelli, O. Atinault, C. François and B. Paluch. Multidisciplinary Design and performance of the ONERA Hybrid Electric Distributed Propulsion concept (DRAGON). AIAA SciTech Forum. AIAA 2020-0501. https://doi.org/10.2514/6.2020-0501.
[22] D.P. Raymer. 2012. Aircraft Design: A conceptual Approach, 5th ed.; AIAA Education Series; American Institute of Aeronautics and Astronautics, Inc.: Reston, VA, USA, 2012; p. 495. ISBN 9781600869112.
[23] A. M. Stoll, G.V. Mikic, Design Studies of Thin-Haul Commuter Aircraft with Distributed Electric Propulsion. *16th AIAA Aviation Technology, Integration, and Operations Conference*. 13-17 June 2016. Washington D.C. USA. https://doi.org/10.2514/6.2016-3765.
[24] MASS tool information. Online: https://www.nlr.org/flyers/en/f543-analyse-the-energy-performance-of-aircraft.pdf. [Accessed 10 June 2022].
[25] Gas turbine Simulation Program, Online: http://www.gspteam.com [Accessed 10 June 2022].
[26] Base of aircraft data. Online: https://www.eurocontrol.int/model/bada [Accessed 10 June 2022].
[27] EUROCONTROL. Taxi times - Winter 2018-2019. Online: https://www.eurocontrol.int/publication/taxi-times-winter-2018-2019 [Accessed 10 June 2022].
[28] EUROCONTROL. Taxi times - Summer 2019. Online: https://www.eurocontrol.int/publication/taxi-times-summer-2019 [Accessed 10 June 2022].
[29] EASA. Emissions Databank - New Format (08/2020). Online: https://www.easa.europa.eu/domains/environment/icao-aircraft-engine-emissions-databank. [Accessed 10 June 2022].
[30] Bjorn Fehrm. 2021. Bjorn's Corner: The challenges of hydrogen. Part 19. Hydrogen airliner weight shift. Leeham News and Analysis January 8. 2021. Online: https://leehamnews.com/2021/01/08/bjorns-corner-the-challenges-of-hydrogen-part-18-hydrogen-airliner-weight-shift/ [Accessed 10 June 2022].
[31] W.F. Lammen, W.J. Vankan. 2020, Energy Optimization of Single Aisle Aircraft with Hybrid Electric Propulsion. *AIAA Scitech 2020 Forum*. Orlando. FL. USA. January 6-10 2020. doi: 10.2514/6.2020-0505. NLR-TP-2020-114.
[32] B. Fehrm. 2020. Bjorn's Corner: The challenges of hydrogen. Part 11. Emissions. Leeham News and Analysis October. 2020. Online: https://leehamnews.com/2020/10/02/34733/ [Accessed 10 June 2022].
[33] L. Blain. 2022. Ultra-light liquid hydrogen tanks promise to make jet fuel obsolete. Online: Ultra-light liquid hydrogen tanks promise to make jet fuel obsolete (newatlas.com) [Accessed 10 June 2022].
[34] J.Kos, J. Posada-Duque, B. Peerlings, N. ben Salah, N. Lim, W. Lammen, I. Stepchuk, E. van der Sman1, M. Palmeros-Parada. Novel aircraft propulsion and availability of alternative, sustainable aviation fuels in 2050. *Submitted to ICAS 2022*.